NIST Special Publication 1018-5

Fire Dynamics Simulator (Version 5) Technical Reference Guide

Volume 2: Verification

Randall McDermott
Kevin McGrattan
Simo Hostikka
Jason Floyd

National Institute of Standards and Technology
U.S. Department of Commerce

NIST Special Publication 1018-5

Fire Dynamics Simulator (Version 5) Technical Reference Guide

Volume 2: Verification

Randall McDermott
Kevin McGrattan
Fire Research Division
Building and Fire Research Laboratory

Simo Hostikka
VTT Technical Research Centre of Finland
Espoo, Finland

Jason Floyd
Hughes Associates, Inc.
Baltimore, Maryland

July 29, 2008
FDS Version 5.2
SVNRepository Revision : 1835

U.S. Department of Commerce
Carlos M. Gutierrez, Secretary

National Institute of Standards and Technology
William A. Jeffrey, Director

Preface

This is Volume 2 of the FDS Technical Reference Guide. Volume 1 describes the mathematical model and numerical method. Volume 3 documents past and present experimental validation work. Instructions for using FDS are contained in a separate User's Guide [1].

The three volumes of the FDS Technical Reference Guide are based in part on the "Standard Guide for Evaluating the Predictive Capability of Deterministic Fire Models," ASTM E 1355 [2]. ASTM E 1355 defines *model evaluation* as "the process of quantifying the accuracy of chosen results from a model when applied for a specific use." The model evaluation process consists of two main components: verification and validation. *Verification* is a process to check the correctness of the solution of the governing equations. Verification does not imply that the governing equations are appropriate; only that the equations are being solved correctly. *Validation* is a process to determine the appropriateness of the governing equations as a mathematical model of the physical phenomena of interest. Typically, validation involves comparing model results with experimental measurement. Differences that cannot be explained in terms of numerical errors in the model or uncertainty in the measurements are attributed to the assumptions and simplifications of the physical model.

Evaluation is critical to establishing both the acceptable uses and limitations of a model. Throughout its development, FDS has undergone various forms of evaluation, both at NIST and beyond. This volume provides a survey of verification work conducted to date to evaluate FDS.

About the Authors

Randall McDermott joined the research staff of the Building and Fire Research Lab in 2008. He received a B.S. degree from the University of Tulsa in Chemical Engineering in 1994 and a doctorate at the University of Utah in 2005. His research interests include domain decomposition, Lagrangian particle methods, and adaptive mesh refinement.

Kevin McGrattan is a mathematician in the Building and Fire Research Laboratory (BFRL) of NIST. He received a bachelors of science degree from the School of Engineering and Applied Science of Columbia University in 1987 and a doctorate at the Courant Institute of New York University in 1991. He joined the NIST staff in 1992 and has since worked on the development of fire models, most notably the Fire Dynamics Simulator.

Simo Hostikka is a Senior Research Scientist at VTT Technical Research Centre of Finland. He received a master of science (technology) degree in 1997 and a doctorate in 2008 from the Department of Engineering Physics and Mathematics of the Helsinki University of Technology. He is the principal developer of the radiation and solid phase sub-models within FDS.

Jason Floyd is a Senior Engineer at Hughes Associates, Inc., in Baltimore, Maryland. He received a bachelors of science and Ph.D. in the Nuclear Engineering Program of the University of Maryland. After graduating, he won a National Research Council Post-Doctoral Fellowship at the Building and Fire Research Laboratory of NIST, where he developed the combustion algorithm within FDS. He is currently funded by NIST under grant 60NANB5D1205 from the Fire Research Grants Program (15 USC 278f). He is the principal developer of the multi-parameter mixture fraction combustion model and control logic within FDS.

Acknowledgments

Partial support for the preparation of the FDS Technical Reference Guides has been provided by the Office of Nuclear Regulatory Research of the US Nuclear Regulatory Commission (US NRC). Special thanks to Mark Salley and Jason Dreisbach for their efforts.

Thanks to Chris Lautenburger and Carlos Fernandez-Pello for their assistance with the “two-reaction” test case.

Contents

Chapter 1

What is Verification?

The terms *verification* and *validation* are often used interchangeably to mean the process of checking the accuracy of a numerical model. For many, this entails comparing model predictions with experimental measurements. However, there is now a fairly broad-based consensus that comparing model and experiment is largely what is considered *validation*. So what is *verification*? ASTM E 1355 [2], "Standard Guide for Evaluating the Predictive Capability of Deterministic Fire Models," defines verification as

> The process of determining that the implementation of a calculation method accurately represents the developer's conceptual description of the calculation method and the solution to the calculation method.

and it defines validation as

> The process of determining the degree to which a calculation method is an accurate representation of the real world from the perspective of the intended uses of the calculation method.

Simply put, verification is a check of the math; validation is a check of the physics. If the model predictions closely match the results of experiments, using whatever metric is appropriate, it is assumed by most that the model suitably describes, via its mathematical equations, what is happening. It is also assumed that the solution of these equations must be correct. So why do we need to perform model verification? Why not just skip to validation and be done with it? The reason is that rarely do model and measurement agree so well in all applications that anyone would just accept its results unquestionably. Because there is inevitably differences between model and experiment, we need to know if these differences are due to limitations or errors in the numerical solution, or the physical sub-models, or both.

Whereas model validation consists mainly of comparing predictions with measurements, as documented for FDS in Volume 3 of the Technical Reference Guide, model verification consists of a much broader range of activities, from checking the computer program itself to comparing calculations to analytical (exact) solutions to considering the sensitivity of the dozens of numerical parameters. The next chapter discusses these various activities, and the rest of the Guide is devoted mainly to comparisons of various sub-model calculations with analytical solutions.

Chapter 2

Survey of Past Verification Work

This chapter documents work of the past few decades at NIST, VTT and elsewhere to verify the algorithms within FDS.

2.1 Analytical Tests

Most complex combustion processes, including fire, are turbulent and time-dependent. There are no closed-form mathematical solutions for the fully-turbulent, time-dependent Navier-Stokes equations. CFD provides an approximate solution for the non-linear partial differential equations by replacing them with discretized algebraic equations that can be solved using a powerful computer. While there is no general analytical solution for fully-turbulent flows, certain sub-models address phenomenon that do have analytical solutions, for example, one-dimensional heat conduction through a solid. These analytical solutions can be used to test sub-models within a complex code such as FDS. The developers of FDS routinely use such practices to verify the correctness of the coding of the model [3, 4]. Such verification efforts are relatively simple and routine and the results may not always be published nor included in the documentation. Examples of routine analytical testing include:

- The radiation solver has been verified with scenarios where simple objects, like cubes or flat plates, are positioned in simple, sealed compartments. All convective motion is turned off, the object is given a fixed surface temperature and emissivity of one (making it a black body radiator). The heat flux to the cold surrounding walls is recorded and compared to analytical solutions. These studies help determine the appropriate number of solid angles to be set as the default.

- Solid objects are heated with a fixed heat flux, and the interior and surface temperatures as a function of time are compared to analytical solutions of the one-dimensional heat transfer equation. These studies help determine the number of nodes to use in the solid phase heat transfer model. Similar studies are performed to check the pyrolysis models for thermoplastic and charring solids.

- Early in its development, the hydrodynamic solver that evolved to form the core of FDS was checked against analytical solutions of simplified fluid flow phenomena. These studies were conducted at the National Bureau of Standards (NBS)[1] by Rehm, Baum and co-workers [5, 6, 7, 8]. The emphasis of this early work was to test the stability and consistency of the basic hydrodynamic solver, especially the velocity-pressure coupling that is vitally important in low Mach number applications. Many numerical algorithms developed up to that point in time were intended for use in high-speed flow applications, like aerospace. Many of the techniques adopted by FDS were originally developed for

[1]The National Institute of Standards and Technology (NIST) was formerly known as the National Bureau of Standards.

meteorological models, and as such needed to be tested to assess whether they would be appropriate to describe relatively low-speed flow within enclosures.

- A fundamental decision made by Rehm and Baum early in the FDS development was to use a direct (rather than iterative) solver for the pressure. In the low Mach number formulation of the Navier-Stokes equations, an elliptic partial differential equation for the pressure emerges, often referred to as the Poisson equation. Most CFD methods use iterative techniques to solve the governing conservation equations to avoid the necessity of directly solving the Poisson equation. The reason for this is that the equation is time-consuming to solve numerically on anything but a rectilinear grid. Because FDS is designed specifically for rectilinear grids, it can exploit fast, direct solvers of the Poisson equation, obtaining the pressure field with one pass through the solver to machine accuracy. FDS employs double-precision (8 byte) arithmetic, meaning that the relative difference between the computed and the exact solution of the discretized Poisson equation is on the order of 10^{-12}. The fidelity of the numerical solution of the entire system of equations is tied to the pressure/velocity coupling because often simulations can involve hundreds of thousands of time steps, with each time step consisting of two solutions of the Poisson equation to preserve second-order accuracy. Without the use of the direct Poisson solver, build-up of numerical error over the course of a simulation could produce spurious results. Indeed, an attempt to use single-precision (4 byte) arithmetic to conserve machine memory led to spurious results simply because the error per time step built up to an intolerable level.

2.2 Numerical Tests

Numerical techniques used to solve the governing equations within a model can be a source of error in the predicted results. The hydrodynamic model within FDS is second-order accurate in space and time. This means that the error terms associated with the approximation of the spatial partial derivatives by finite differences is of the order of the square of the grid cell size, and likewise the error in the approximation of the temporal derivatives is of the order of the square of the time step. As the numerical grid is refined, the “discretization error” decreases, and a more faithful rendering of the flow field emerges. The issue of grid sensitivity is extremely important to the proper use of the model and will be taken up in the next chapter.

A common technique of testing flow solvers is to systematically refine the numerical grid until the computed solution does not change, at which point the calculation is referred to as a Direct Numerical Solution (DNS) of the governing equations. For most practical fire scenarios, DNS is not possible on conventional computers. However, FDS does have the option of running in DNS mode, where the Navier-Stokes equations are solved without the use of sub-grid scale turbulence models of any kind. Because the basic numerical method is the same for LES and DNS, DNS calculations are a very effective way to test the basic solver, especially in cases where the solution is steady-state. Throughout its development, FDS has been used in DNS mode for special applications. For example, FDS (or its core algorithms) have been used at a grid resolution of roughly 1 mm to look at flames spreading over paper in a microgravity environment [9, 10, 11, 12, 13, 14], as well as "g-jitter" effects aboard spacecraft [15]. Simulations have been compared to experiments performed aboard the US Space Shuttle. The flames are laminar and relatively simple in structure, and the comparisons are a qualitative assessment of the model solution. Similar studies have been performed comparing DNS simulations of a simple burner flame to laboratory experiments [16]. Another study compared FDS simulations of a counterflow diffusion flames to experimental measurements and the results of a one-dimensional multi-step kinetics model [17].

Early work with the hydrodynamic solver compared two-dimensional simulations of gravity currents with salt-water experiments [18]. In these tests, the numerical grid was systematically refined until almost perfect agreement with experiment was obtained. Such convergence would not be possible if there were a fundamental flaw in the hydrodynamic solver.

2.3 Sensitivity Analysis

A sensitivity analysis considers the extent to which uncertainty in model inputs influences model output. Model parameters can be the physical properties of solids and gases, boundary conditions, initial conditions, *etc.* The parameters can also be purely numerical, like the size of the numerical grid. FDS typically requires the user to provide several dozen different types of input parameters that describe the geometry, materials, combustion phenomena, *etc.* By design, the user is not expected to provide numerical parameters besides the grid size, although the optional numerical parameters are described in both the Technical Reference Guide and the User's Guide.

FDS does not limit the range of most of the input parameters because applications often push beyond the range for which the model has been validated. FDS is still used for research at NIST and elsewhere, and the developers do not presume to know in all cases what the acceptable range of any parameter is. Plus, FDS solves the fundamental conservation equations and is much less susceptible to errors resulting from input parameters that stray beyond the limits of simpler empirical models. However, the user is warned that he/she is responsible for the prescription of all parameters. The FDS manuals can only provide guidance.

The grid size is the most important numerical parameter in the model, as it dictates the spatial and temporal accuracy of the discretized partial differential equations. The heat release rate is the most important physical parameter, as it is the source term in the energy equation. Property data, like the thermal conductivity, density, heat of vaporization, heat capacity, *etc.*, ought to be assessed in terms of their influence on the heat release rate. Validation studies have shown that FDS predicts well the transport of heat and smoke when the HRR is prescribed. In such cases, minor changes in the properties of bounding surfaces do not have a significant impact on the results. However, when the HRR is not prescribed, but rather predicted by the model using the thermophysical properties of the fuels, the model output is sensitive to even minor changes in these properties.

The sensitivity analyses described in this chapter are all performed in basically the same way. For a given scenario, best estimates of all the relevant physical and numerical parameters are made, and a "baseline" simulation is performed. Then, one by one, parameters are varied by a given percentage, and the changes in predicted results are recorded. This is the simplest form of sensitivity analysis. More sophisticated techniques that involve the simultaneous variation of several parameters are impractical with a CFD model because the computation time is too long and the number of parameters too large to perform the necessary number of calculations to generate decent statistics.

2.3.1 Grid Sensitivity

The most important decision made by a model user is the size of the numerical grid. In general, the finer the numerical grid, the better the numerical solution of the equations. FDS is second-order accurate in space and time, meaning that halving the grid cell size will decrease the discretization error in the governing equations by a factor of 4. Because of the non-linearity of the equations, the decrease in discretization error does not necessarily translate into a comparable decrease in the error of a given FDS output quantity. To find out what effect a finer grid has on the solution, model users usually perform some form of grid sensitivity study in which the numerical grid is systematically refined until the output quantities do not change appreciably with each refinement. Of course, with each halving of the grid cell size, the time required for the simulation increases by a factor of $2^4 = 16$ (a factor of two for each spatial coordinate, plus time). In the end, a compromise is struck between model accuracy and computer capacity.

Some grid sensitivity studies have been documented and published. Since FDS was first publicly released in 2000, significant changes in the combustion and radiation routines have been incorporated into the model. However, the basic transport algorithm is the same, as is the critical importance of grid sensitivity. In compiling sensitivity studies, only those that examined the sensitivity of routines no longer used have been excluded.

As part of a project to evaluate the use of FDS version 1 for large scale mechanically ventilated enclosures, Friday [19] performed a sensitivity analysis to find the approximate calculation time based on varying grid sizes. A propylene fire with a nominal heat release rate was modeled in FDS. There was no mechanical ventilation and the fire was assumed to grow as a function of the time from ignition squared. The compartment was a 3 m by 3 m by 6.1 m space. Temperatures were sampled 12 cm below the ceiling. Four grid sizes were chosen for the analysis: 30 cm, 15 cm, 10 cm, 7.5 cm. Temperature estimates were not found to change dramatically with different grid dimensions.

Using FDS version 1, Bounagui *et al.* [20] studied the effect of grid size on simulation results to determine the nominal grid size for future work. A propane burner 0.1 m by 0.1 m was modeled with a heat release rate of 1500 kW. A similar analysis was performed using Alpert's ceiling jet correlation [21] that also showed better predictions with smaller grid sizes. In a related study, Bounagui *et al.* [22] used FDS to evaluate the emergency ventilation strategies in the Louis-Hippolyte-La Fontaine Tunnel in Montreal, Canada.

Xin [23] used FDS to model a methane fueled square burner (1 m by 1 m) in the open. Engineering correlations for plume centerline temperature and velocity profiles were compared with model predictions to assess the influence of the numerical grid and the size of the computational domain. The results showed that FDS is sensitive to grid size effects, especially in the region near the fuel surface, and domain size effects when the domain width is less than twice the plume width. FDS uses a constant pressure assumption at open boundaries. This assumption will affect the plume behavior if the boundary of the computational domain is too close to the plume.

Ierardi and Barnett [24] used FDS version 3 to model a 0.3 m square methane diffusion burner with heat release rate values in the range of 14.4 kW to 57.5 kW. The physical domain used was 0.6 m by 0.6 m with uniform grid spacings of 15, 10, 7.5, 5, 3, 1.5 cm for all three coordinate directions. For both fire sizes, a grid spacing of 1.5 cm was found to provide the best agreement when compared to McCaffrey's centerline plume temperature and velocity correlations [25]. Two similar scenarios that form the basis for Alpert's ceiling jet correlation were also modeled with FDS. The first scenario was a 1 m by 1 m, 670 kW ethanol fire under a 7 m high unconfined ceiling. The planar dimensions of the computational domain were 14 m by 14 m. Four uniform grid spacings of 50, 33.3, 25, and 20 cm were used in the modeling. The best agreement for maximum ceiling jet temperature was with the 33.3 cm grid spacing. The best agreement for maximum ceiling jet velocity was for the 50 cm grid spacing. The second scenario was a 0.6 m by 0.6 m 1000 kW ethanol fire under a 7.2 m high unconfined ceiling. The planar dimensions of the computational domain were 14.4 m by 14.4 m. Three uniform grid spacings of 60, 30, and 20 cm were used in the modeling. The results show that the 60 cm grid spacing exhibits the best agreement with the correlations for both maximum ceiling jet temperature and velocity on a qualitative basis.

Petterson [26] also completed work assessing the optimal grid size for FDS version 2. The FDS model predictions of varying grid sizes were compared to two separate fire experiments: The University of Canterbury McLeans Island Tests and the US Navy Hangar Tests in Hawaii. The first set of tests utilized a room with approximate dimensions of 2.4 m by 3.6 m by 2.4 m and fire sizes of 55 kW and 110 kW. The Navy Hangar tests were performed in a hangar measuring 98 m by 74 m by 15 m in height and had fires in the range of 5.5 MW to 6.6 MW. The results of this study indicate that FDS simulations with grids of 0.15 m had temperature predictions as accurate as models with grids as small as 0.10 m. Each of these grid sizes produced results within 15 % of the University of Canterbury temperature measurements. The 0.30 m grid produced less accurate results. For the comparison of the Navy Hangar tests, grid sizes ranging from 0.60 m to 1.80 m yielded results of comparable accuracy.

Musser *et al.* [27] investigated the use of FDS for course grid modeling of non-fire and fire scenarios. Determining the appropriate grid size was found to be especially important with respect to heat transfer at heated surfaces. The convective heat transfer from the heated surfaces was most accurate when the near surface grid cells were smaller than the depth of the thermal boundary layer. However, a finer grid size produced better results at the expense of computational time. Accurate contaminant dispersal modeling required a significantly finer grid. The results of her study indicate that non-fire simulations can be completed more quickly than fire simulations because the time step is not limited by the large flow speeds in a fire plume.

2.3.2 Sensitivity of Large Eddy Simulation Parameters

FDS uses the Smagorinsky form of the Large Eddy Simulation (LES) technique. This means that instead of using the actual fluid viscosity, the model uses a viscosity of the form

$$\mu_{\mathrm{LES}} = \rho\,(C_s\,\Delta)^2\,|S|^{\frac{1}{2}} \tag{2.1}$$

where C_s is an empirical constant, Δ is a length on the order of the size of a grid cell, and the deformation term $|S|$ is related to the Dissipation Function (see FDS Technical Reference Guide [28] for details). Related to the "turbulent viscosity" are comparable expressions for the thermal conductivity and material diffusivity:

$$k_{\mathrm{LES}} = \frac{\mu_{\mathrm{LES}}\,c_p}{\mathrm{Pr}} \quad ; \quad (\rho D)_{\mathrm{LES}} = \frac{\mu_{\mathrm{LES}}}{\mathrm{Sc}} \tag{2.2}$$

The Prandtl number Pr and the Schmidt number Sc are likewise considered to be "turbulent" values. Thus, C_s, Pr and Sc are a set of empirical constants. Most FDS users simply use the default values of (0.2,0.5,0.5), but some have explored their effect on the solution of the equations.

In an effort to validate FDS with some simple room temperature data, Zhang *et al.* [29] tried different combinations of the Smagorinsky parameters, and suggested the current default values. Of the three parameters, the Smagorinsky constant C_s is the most sensitive. Smagorinsky [30] originally proposed a value of 0.23, but researchers over the past three decades have used values ranging from 0.1 to 0.23. There are also refinements of the original Smagorinsky model [31, 32, 33] that do not require the user to prescribe the constants, but rather generate them automatically as part of the numerical scheme.

2.3.3 Sensitivity of Radiation Parameters

Radiative heat transfer is included in FDS via the solution of the radiation transport equation for a non-scattering gray gas, and in some limited cases using a wide band model. The equation is solved using a technique similar to finite volume methods for convective transport, thus the name given to it is the Finite Volume Method (FVM). There are several limitations of the model. First, the absorption coefficient for the smoke-laden gas is a complex function of its composition and temperature. Because of the simplified combustion model, the chemical composition of the smokey gases, especially the soot content, can effect both the absorption and emission of thermal radiation. Second, the radiation transport is discretized via approximately 100 solid angles. For targets far away from a localized source of radiation, like a growing fire, the discretization can lead to a non-uniform distribution of the radiant energy. This can be seen in the visualization of surface temperatures, where "hot spots" show the effect of the finite number of solid angles. The problem can be lessened by the inclusion of more solid angles, but at a price of longer computing times. In most cases, the radiative flux to far-field targets is not as important as those in the near-field, where coverage by the default number of angles is much better.

Hostikka *et al.* examined the sensitivity of the radiation solver to changes in the assumed soot production, number of spectral bands, number of control angles, and flame temperature. Some of the more interesting findings were:

- Changing the soot yield from 1 % to 2 % increased the radiative flux from a simulated methane burner about 15 %

- Lowering the soot yield to zero decreased the radiative flux about 20 %.
- Increasing the number of control angles by a factor of 3 was necessary to ensure the accuracy of the model at the discrete measurement locations.
- Changing the number of spectral bands from 6 to 10 did not have a strong effect on the results.
- Errors of 100 % in heat flux were caused by errors of 20 % in absolute temperature.

The sensitivity to flame temperature and soot composition are consistent with combustion theory, which states that the source term of the radiative transport equation is a function of the absorption coefficient multiplied by the absolute temperature raised to the fourth power. The number of control angles and spectral bands are user-controlled numerical parameters whose sensitivities ought to be checked for each new scenario. The default values in FDS are appropriate for most large scale fire scenarios, but may need to be refined for more detailed simulations such as a low-sooting methane burner.

2.3.4 Sensitivity of Thermophysical Properties of Solid Fuels

An extensive amount of verification and validation work with FDS version 4 has been performed by Hietaniemi, Hostikka, and Vaari at VTT, Finland [34]. The case studies are comprised of fire experiments ranging in scale from the cone calorimeter (ISO 5660-1) to full-scale fire tests such as the room corner test (ISO 9705). Comparisons are also made between FDS results and data obtained in the SBI (Single Burning Item) Euro-classification test apparatus (EN 13823) as well as data obtained in two *ad hoc* experimental configurations: one is similar to the room corner test but has only partial linings and the other is a space to study fires in building cavities.

All of the case studies involve real materials whose properties must be prescribed so as to conform to the assumption in FDS that solids are of uniform composition backed by a material that is either cold or totally insulating. Sensitivity of the various physical properties and the boundary conditions were tested. Some of the findings were:

- The measured burning rates of various materials often fell between two FDS predictions in which cold or insulated backings were assumed for the solid surfaces. FDS lacks a multi-layer solid model.
- The ignition time of upholstery is sensitive to the thermal properties of the fabric covering, but the steady burning rate is sensitive to the properties of the underlying foam.
- Moisture content of wooden fuels is very important and difficult to measure.
- Flame spread over complicated objects, like cables laid out in trays, can be modeled if the surface area of the simplified object is comparable to that of the real object. This suggests sensitivity not only to physical properties, but also geometry. It is difficult to quantify the extent of the geometrical sensitivity.

There is little quantification of the observed sensitivities in the study. Fire growth curves can be linear to exponential in form, and small changes in fuel properties can lead to order of magnitude changes in heat release rate for unconfined fires. The subject is discussed in the FDS Validation Guide (Volume 3 of the Technical Reference Guide). where it is noted in many of the studies that predicting fire growth is difficult.

Recently, Lautenberger, Rein and Fernandez-Pello [35] developed a method to automate the process of estimating material properties to input into FDS. The methodology involves simulating a bench-scale test with the model and iterating via a "genetic" algorithm to obtain an optimal set of material properties for that particular item. Such techniques are necessary because most bench-scale apparatus do not provide a complete set of thermal properties.

2.4 Code Checking

An examination of the structure of the computer program can be used to detect potential errors in the numerical solution of the governing equations. The coding can be verified by a third party either manually or automatically with profiling programs to detect irregularities and inconsistencies [2].

At NIST and elsewhere, FDS has been compiled and run on computers manufactured by IBM, Hewlett-Packard, Sun Microsystems, Digital Equipment Corporation, Apple, Silicon Graphics, Dell, Compaq, and various other personal computer vendors. The operating systems on these platforms include Unix, Linux, Microsoft Windows, and Mac OSX. Compilers used include Lahey Fortran, Digital Visual Fortran, Intel Fortran, IBM XL Fortran, HPUX Fortran, Forte Fortran for SunOS, the Portland Group Fortran, and several others. Each combination of hardware, operating system and compiler involves a slightly different set of compiler and run-time options and a rigorous evaluation of the source code to test its compliance with the Fortran 90 ISO/ANSI standard [36]. Through this process, out-dated and potentially harmful code is updated or eliminated, and often the code is streamlined to improve its optimization on the various machines. However, simply because the FDS source code can be compiled and run on a wide variety of platforms does not guarantee that the numerics are correct. It is only the starting point in the process because it at least rules out the possibility that erratic or spurious results are due to the platform on which the code is running.

Beyond hardware issues, there are several useful techniques for checking the FDS source code that have been developed over the years. One of the best ways is to exploit symmetry. FDS is filled with thousands of lines of code in which the partial derivatives in the conservation equations are approximated as finite differences. It is very easy in this process to make a mistake. Consider, for example, the finite difference approximation of the thermal diffusion term in the ijkth cell of the three-dimensional grid:

$$
\begin{aligned}
(\nabla\cdot k\nabla T)_{ijk} \;\approx\;& \frac{1}{\delta x}\left[k_{i+\frac{1}{2},jk}\frac{T_{i+1,jk}-T_{ijk}}{\delta x}-k_{i-\frac{1}{2},jk}\frac{T_{ijk}-T_{i-1,jk}}{\delta x}\right]+\\
& \frac{1}{\delta y}\left[k_{i,j+\frac{1}{2},k}\frac{T_{i,j+1,k}-T_{ijk}}{\delta y}-k_{i,j-\frac{1}{2},k}\frac{T_{ijk}-T_{i,j-1,k}}{\delta y}\right]+\\
& \frac{1}{\delta z}\left[k_{ij,k+\frac{1}{2}}\frac{T_{ij,k+1}-T_{ijk}}{\delta z}-k_{ij,k-\frac{1}{2}}\frac{T_{ijk}-T_{ij,k-1}}{\delta z}\right]
\end{aligned}
$$

which is written as follows in the Fortran source code:

```
DTDX = (TMP(I+1,J,K)-TMP(I,J,K))*RDXN(I)
KDTDX(I,J,K) = .5*(KP(I+1,J,K)+KP(I,J,K))*DTDX
DTDY = (TMP(I,J+1,K)-TMP(I,J,K))*RDYN(J)
KDTDY(I,J,K) = .5*(KP(I,J+1,K)+KP(I,J,K))*DTDY
DTDZ = (TMP(I,J,K+1)-TMP(I,J,K))*RDZN(K)
KDTDZ(I,J,K) = .5*(KP(I,J,K+1)+KP(I,J,K))*DTDZ

DELKDELT = (KDTDX(I,J,K)-KDTDX(I-1,J,K))*RDX(I) +
.            (KDTDY(I,J,K)-KDTDY(I,J-1,K))*RDY(J) +
.            (KDTDZ(I,J,K)-KDTDZ(I,J,K-1))*RDZ(K)
```

This is one of the simpler constructs because the pattern that emerges within the lines of code make it fairly easy to check. However, a mis-typing of an `I` or a `J`, a plus or a minus sign, or any of a hundred different mistakes can cause the code to fail, or worse produce the wrong answer. A simple way to eliminate many of these mistakes is to run simple scenarios that have perfectly symmetric initial and boundary conditions. For example, put a hot cube in the exact center of a larger cold compartment, turn off gravity, and watch the heat diffuse from the hot cube into the cold gas. Any simple error in the coding of the energy equation will show up almost immediately. Then, turn on gravity, and in the absence of any coding error, a perfectly symmetric plume will rise from the hot cube. This checks both the coding of the energy and the momentum equations. Similar checks can be made for all of the three dimensional finite difference routines. So extensive are these types of checks that the release version of FDS has a routine that generates a tiny amount of random noise in the initial flow field so as to eliminate any false symmetries that might arise in the numerical solution.

The process of adding new routines to FDS is as follows: typically the routine is written by one person (not necessarily a NIST staffer) who takes the latest version of the source code, adds the new routine, and writes a theoretical and numerical description for the FDS Technical Reference Guide, plus a description of the input parameters for the FDS User's Guide. The new version of FDS is then tested at NIST with a number of benchmark scenarios that exercise the range of the new parameters. Provisional acceptance of the new routine is based on several factors: (1) it produces more accurate results when compared to experimental measurement, (2) the theoretical description is sound, and (3) any empirical parameters are obtainable from the open literature or standard bench-scale apparatus. If the new routine is accepted, it is added to a test version of the software and evaluated by external users and/or NIST grantees whose research is related to the subject. Assuming that there are no intractable issues that arise during the testing period, the new routine eventually becomes part of the release version of FDS.

Even with all the code checking performed at NIST, it is still possible for errors to go unnoticed. One remedy is the fact that the source code for FDS is publicly released. Although it consists of on the order of 30,000 lines of Fortran statements, various researchers outside of NIST have been able to work with it, add enhancements needed for very specific applications or for research purposes, and report back to the developers bugs that have been detected. The source code is organized into 27 separate files, each containing subroutines related to a particular feature of the model, like the mass, momentum, and energy conservation equations, sprinkler activation and sprays, the pressure solver, *etc.* The lengthiest routines are devoted to input, output and initialization. Most of those working with the source code do not concern themselves with these lengthy routines but rather focus on the finite-difference algorithm contained in a few of the more important files. Most serious errors are found in these files, for they contain the core of the algorithm. The external researchers provide feedback on the organization of the code and its internal documentation, that is, comments within the source code itself. Plus, they must compile the code on their own computers, adding to its portability.

Chapter 3

Thermal Radiation

The Radiative Transport Equation (RTE) for an absorbing/emitting and scattering medium is

$$\mathbf{s}\cdot\nabla I_\lambda(\mathbf{x},\mathbf{s}) = -\left[\kappa(\mathbf{x},\lambda)+\sigma_s(\mathbf{x},\lambda)\right] I_\lambda(\mathbf{x},\mathbf{s}) + B(\mathbf{x},\lambda) + \frac{\sigma_s(\mathbf{x},\lambda)}{4\pi}\int_{4\pi}\Phi(\mathbf{s},\mathbf{s}')\, I_\lambda(\mathbf{x},\mathbf{s}')\, d\mathbf{s}' \tag{3.1}$$

where $I_\lambda(\mathbf{x},\mathbf{s})$ is the radiation intensity at wavelength λ, $\mathbf{s}$ is the direction vector of the intensity, $\kappa(\mathbf{x},\lambda)$ and $\sigma_s(\mathbf{x},\lambda)$ are the local absorption and scattering coefficients, respectively, and $B(\mathbf{x},\lambda)$ is the emission source term. The integral on the right hand side describes the in-scattering from other directions. In the case of a non-scattering gas the RTE becomes

$$\mathbf{s}\cdot\nabla I_\lambda(\mathbf{x},\mathbf{s}) = \kappa(\mathbf{x},\lambda)\,\left[I_b(\mathbf{x}) - I_\lambda(\mathbf{x},\mathbf{s})\right] \tag{3.2}$$

where $I_b(\mathbf{x})$ is the source term given by the Planck function (see below).

In practical simulations the spectral (λ) dependence cannot be solved accurately. Instead, the radiation spectrum is divided into a relatively small number of bands and a separate RTE is derived for each band. The band specific RTE is

$$\mathbf{s}\cdot\nabla I_n(\mathbf{x},\mathbf{s}) = \kappa_n(\mathbf{x})\;\left[I_{b,n}(\mathbf{x}) - I_n(\mathbf{x},\mathbf{s})\right],\;\; n=1\ldots N \tag{3.3}$$

where I_n is the intensity integrated over the band n, and κ_n is the appropriate mean absorption coefficient inside the band. The source term can be written as a fraction of the blackbody radiation

$$I_{b,n} = F_n(\lambda_{\min},\lambda_{\max})\;\sigma\, T^4/\pi \tag{3.4}$$

where σ is the Stefan-Boltzmann constant. The calculation of factors F_n is explained in Ref. [37]. When the intensities corresponding to the bands are known, the total intensity is calculated by summing over all the bands

$$I(\mathbf{x},\mathbf{s}) = \sum_{n=1}^{N} I_n(\mathbf{x},\mathbf{s}) \tag{3.5}$$

There are numerous examples in the heat transfer literature of exact solutions, for simple configurations of hot and cold objects, of the radiation transport equation.

3.1 Radiation inside a box (radiation_in_a_box)

This verification case tests the computation of three-dimensional configuration factor Φ inside a cube box with one hot wall and five cold (0 K) walls. An overview of the test geometry is shown here:

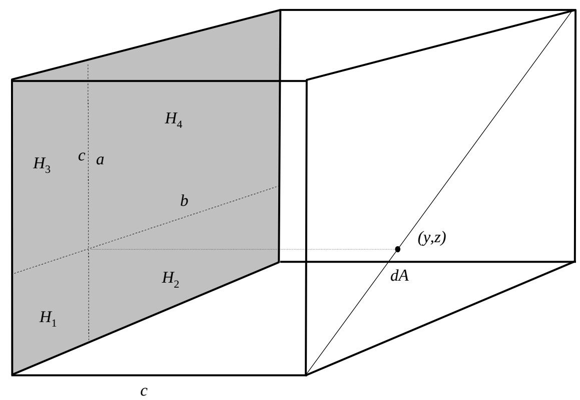

The configuration factors are calculated at the diagonal of the cold wall opposite to the hot wall. The exact values of the configuration factor from plane element dA to parallel rectangle H are calculated using the analytical solution [37]

(y,z)	Φ_{HdA}	(y,z)	Φ_{HdA}
0.025	0.1457	0.275	0.2135
0.075	0.1603	0.325	0.2233
0.125	0.1748	0.375	0.2311
0.175	0.1888	0.425	0.2364
0.225	0.2018	0.475	0.2391

Different variations of the case include the mesh resolution (20^3 and 100^3 cells) and the number of radiation angles (50, 100, 300, 1000, 2000). The exact and FDS results are shown here:

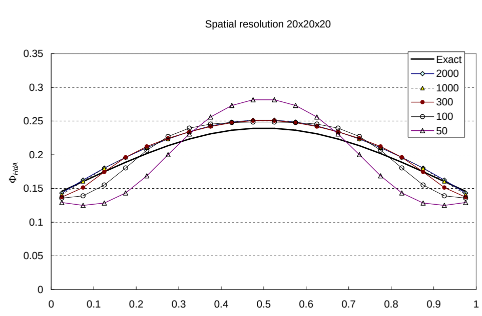

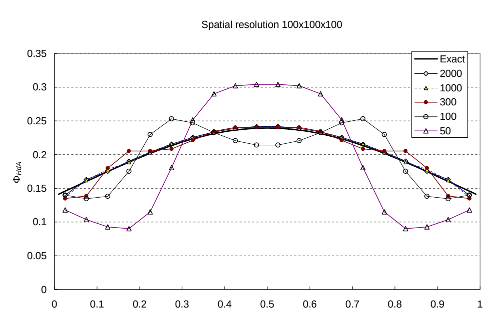

3.2 Radiation from a plane layer (radiation_plane_layer)

This case tests the computation of three-dimensional radiation from a homogenous, infinitely wide layer of hot gases. The temperature of the layer is 1273.15 K and the absorption coefficient, κ, is varied. The thickness of the layer is fixed at 1 m, and the optical depth is $\tau = (1\,\kappa)$ m^{-1}. Wall temperatures are set to 0 K. The results are compared against the exact solution $S(\tau)$ presented in [38]

$$S(\tau) = S_b\,[1 - 2E_3(\tau)] \tag{3.6}$$

where $S_b = \sigma T^4$ is the black-body heat flux from the radiating plane and $E_3(\tau)$ is the exponential integral function (order 3) of the optical depth τ.

The FDS results are computed at two mesh resolutions in the x-direction (I=20 and I=150). For I=20, both one-band and six-band versions are included to test the correct integration of heat fluxes over multiple bands. For I=20, 2-D versions are also computed (J=1). The limiting case, $\tau = \infty$, using a solid wall of temperature 1273.15 K, is computed to test the wall heat flux computation. The exact values and FDS predictions of the wall heat fluxes are given in the table below.

τ	$S(\tau)$	FDS (I=20,J=20)		FDS (I=20,J=1)		FDS (I=150)
(m^{-1})	(kW/m^2)	1 band	6 bands	1 band	6 bands	1 band
0.01	2.8970	2.9180	2.9069	2.8364	2.8256	2.9258
0.1	24.9403	25.5501	25.4529	25.1078	25.0122	25.7045
0.5	82.9457	83.1309	82.8144	84.3719	84.0506	84.0264
1.0	116.2891	115.4051	114.9656	117.801	117.353	116.7751
10.	148.9698	148.9616	148.3947	148.9677	148.4005	148.9695
∞	148.9709	148.9709	148.4037	147.9426	147.3793	148.9709

3.3 Wall Internal Radiation (wall_internal_radiation)

In-depth absorption of thermal radiation in a solid is computed using a two-flux model. In this example, the accuracy of the two-flux model is tested in the computation of the emissive flux from a 0.10 m thick, homogenous layer of material at a temperature of 1273.15 K surrounded by an ambient temperature of 10 K. The absorption coefficient is varied to cover a range [0.01, 10] of optical depth, τ.

The exact solutions for radiative flux are the analytical solutions of plane layer emission [38]

$$S(\tau) = S_b\,[1 - 2E_3(\tau)] \tag{3.7}$$

where $S_b = \sigma T^4$ is the black-body heat flux from the radiating plane and $E_3(\tau)$ is the exponential integral function (order 3) of optical depth, τ. The exact solutions and FDS results are shown in the table below.

τ (m^{-1})	$S(\tau)$ (kW/m^2)	FDS (kW/m^2)
0.01	2.897	2.950
0.1	24.94	26.98
0.5	82.95	93.90
1.0	116.3	128.4
10.	149.0	149.0

Chapter 4

Heat Conduction

This chapter contains examples that test the one-dimensional heat conduction solver in FDS. A one-dimensional heat conduction equation for the solid phase temperature $T_s(x,t)$ is applied in the direction x pointing into the solid (the point $x = 0$ represents the surface)

$$\rho_s c_s \frac{\partial T_s}{\partial t} = \frac{\partial}{\partial x} k_s \frac{\partial T_s}{\partial x} + \dot{q}_s''' \tag{4.1}$$

In cylindrical and spherical coordinates, the heat conduction equation is written

$$\rho_s c_s \frac{\partial T_s}{\partial t} = \frac{1}{r} \frac{\partial}{\partial r} \left(r k_s \frac{\partial T_s}{\partial r} \right) + \dot{q}_s''' \quad ; \quad \rho_s c_s \frac{\partial T_s}{\partial t} = \frac{1}{r^2} \frac{\partial}{\partial r} \left(r^2 k_s \frac{\partial T_s}{\partial r} \right) + \dot{q}_s''' \tag{4.2}$$

FDS offers the user these options, with the assumption that the obstruction is not actually recti-linear, but rather cylindrical or spherical in shape. This option is useful in describing the behavior of small, complicated "targets" like cables or heat detection devices.

4.1 Simple Heat Conduction Through a Solid Slab (heat_conduction)

Analytical solutions of transient, one-dimensional heat conduction through a slab can be found in Refs. [39] and [40]. Four cases are examined here. In each, a slab of thickness $L = 0.1$ m is exposed on one face to an air temperature of $T_g = 120$ °C. The other face is insulated (adiabatic). The convective heat transfer from the gas to the slab is $\dot{q}_c'' = h\,(T_g - T_s)$, where h is constant, and T_s is the slab face temperature. No thermal radiation is included.

Case	k (W/m/K)	ρ (kg/m^3)	c (kJ/kg/K)	h (W/m^2/K)	Bi hL/k
A	0.1	100	1	100	100
B	0.1	100	1	10	10
C	1.0	1000	1	10	1
D	10.0	10000	1	10	0.1

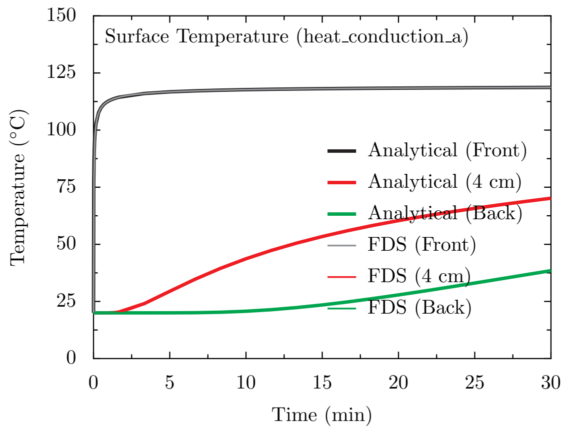

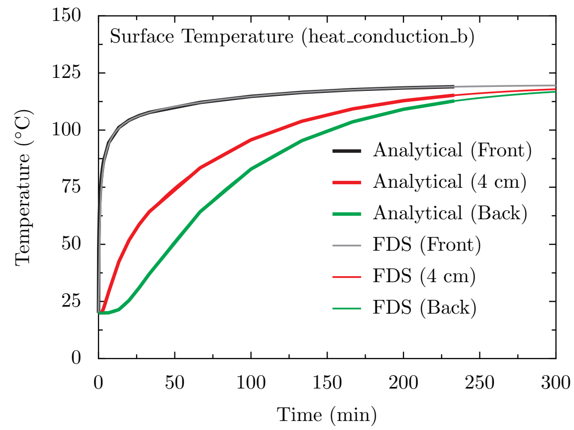

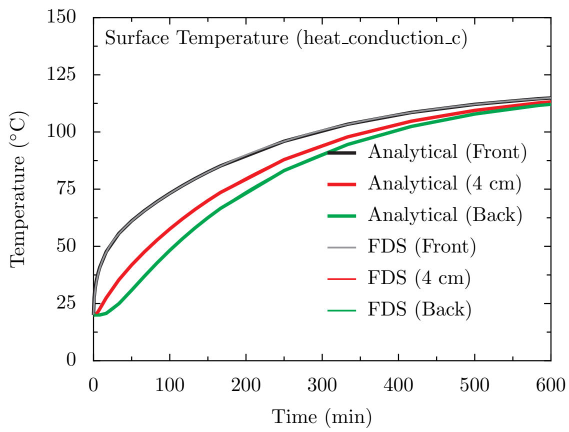

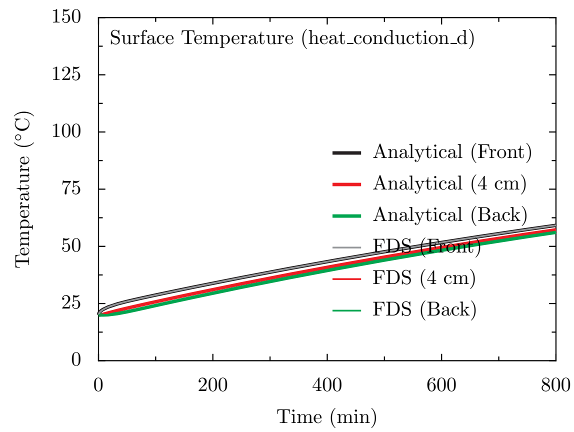

4.2 Temperature-Dependent Thermal Properties (heat_conduction_kc)

This example demonstrates the 1-D heat conduction in cartesian, cylindrical and spherical geometries with temperature-dependent thermal properties. The cartesian solution was computed using HEATING (version 7.3), a multi-dimensional, finite-difference, general purpose heat transfer model [41]. The cylindrical and spherical solutions were computed using a commercial finite-element solver, ABAQUS.

The sample of homogenous material is initially at 0 °C and at $t > 0$ exposed to a gas at 700 °C. A fixed heat transfer coefficient of 10 W/m^2/K is assumed. The density of the material is 10000 kg/m^3. The conductivity and specific heat are functions of temperature with the following values: $k(0) = 0.10$ W/m/K, $k(200) = 0.20$ W/m/K, $c(0) = 1.0$ kJ/kg/K, $c(100) = 1.2$ kJ/kg/K, $c(200) = 1.0$ kJ/kg/K. The thickness (radius) of the sample is 0.01 m. In the cartesian case, the back surface of the material is exposed to a gas at 0 °C. In the figure below, the light colored solid lines are FDS results and the dark lines are the HEATING results. An example input with cylindrical geometry looks like:

```
&MATL ID='MAT_1'
      EMISSIVITY = 0.0
      CONDUCTIVITY_RAMP='K_RAMP'
      SPECIFIC_HEAT_RAMP = 'C_RAMP'
      DENSITY=10000. /

&RAMP ID = 'K_RAMP' T=0,   F= 0.10 /
&RAMP ID = 'K_RAMP' T=100, F= 0.15 /
&RAMP ID = 'K_RAMP' T=200, F= 0.20 /
&RAMP ID = 'C_RAMP' T=0,   F= 1.00 /
&RAMP ID = 'C_RAMP' T=100, F= 1.20 /
&RAMP ID = 'C_RAMP' T=200, F= 1.00 /

&SURF ID='SLAB'
      STRETCH_FACTOR = 1.0
      GEOMETRY = 'CYLINDRICAL'
      MATL_ID='MAT_1'
      THICKNESS=0.01 /
```

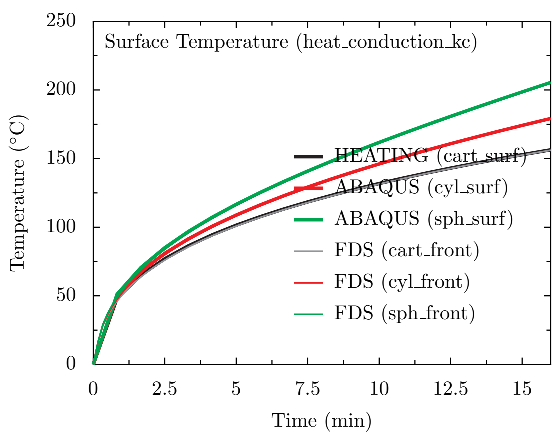

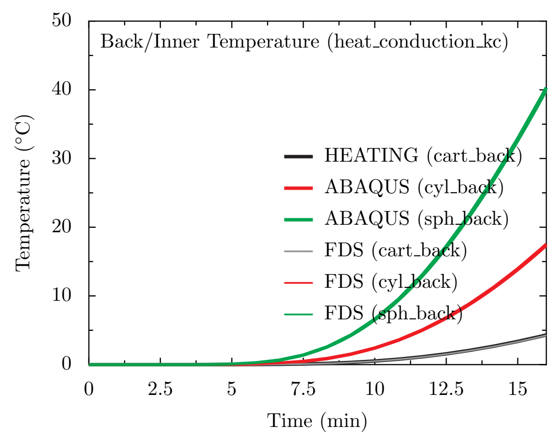

Chapter 5

Pyrolysis

Solids can undergo simultaneous reactions under the following assumptions:

- instantaneous release of volatiles from solid to the gas phase,
- local thermal equilibrium between the solid and the volatiles,
- no condensation of gaseous products, and
- no porosity effects

Each material component may undergo several competing reactions, and each of these reactions may produce some other solid component (residue), gaseous fuel, and/or water vapor according to the yield coefficients ν_s, ν_f and ν_w, respectively. These coefficients should usually satisfy $\nu_s + \nu_f + \nu_w = 1$, but smaller yields may also be used to take into account the gaseous products that are not explicitly included in the simulation.

5.1 A Simple Two-Step Pyrolysis Example (two_step_solid_reaction)

Consider the set of ordinary differential equations describing the mass fraction of three components of a solid material undergoing thermal degradation:

$$\begin{aligned} \frac{dY_a}{dt} &= -K_{ab} Y_a \\ \frac{dY_b}{dt} &= K_{ab} Y_a - K_{bc} Y_b \\ \frac{dY_c}{dt} &= K_{bc} Y_a \end{aligned} \tag{5.1}$$

where the mass fraction of component a is 1 initially. The analytical solution is:

$$Y_a(t) = \exp(-K_{ab} t)$$

$$Y_b(t) = \frac{K_{ab}}{K_{bc} - K_{ab}} \exp(-K_{ab} t) - \exp(-K_{bc} t) \tag{5.2}$$

$$Y_c(t) = \left[K_{ab}(1 - \exp(-K_{bc} t)) + K_{bc} * (\exp(-K_{ab} t) - 1)\right] / (K_{ab} - K_{bc}) \tag{5.3}$$

The analytical and numerical solution for the parameters $K_{ab} = 0.389$ and $K_{bc} = 0.262$ are shown here:

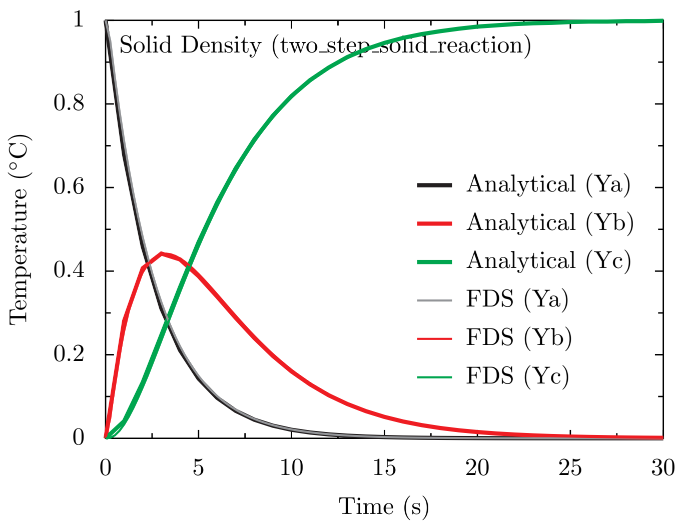

Bibliography

[1] K.B. McGrattan, B.W. Klein, S. Hostikka, and J.E. Floyd. Fire Dynamics Simulator (Version 5), User's Guide. NIST Special Publication 1019-5, National Institute of Standards and Technology, Gaithersburg, Maryland, October 2007. i

[2] American Society for Testing and Materials, West Conshohocken, Pennsylvania. *ASTM E 1355-04, Standard Guide for Evaluating the Predictive Capabilities of Deterministic Fire Models*, 2004. i, 1, 9

[3] W. Mell, K.B. McGrattan, and H. Baum. Numerical Simulation of Combustion in Fire Plumes. In *Twenty-Sixth Symposium (International) on Combustion*, pages 1523–1530. Combustion Institute, Pittsburgh, Pennsylvania, 1996. 3

[4] K.B. McGrattan, H.R. Baum, and R.G. Rehm. Large Eddy Simulations of Smoke Movement. *Fire Safety Journal*, 30:161–178, 1998. 3

[5] H.R. Baum, R.G. Rehm, P.D. Barnett, and D.M. Corley. Finite Difference Calculations of Buoyant Convection in an Enclosure, Part I: The Basic Algorithm. *SIAM Journal of Scientific and Statistical Computing*, 4(1):117–135, March 1983. 3

[6] H.R. Baum and R.G. Rehm. Finite Difference Solutions for Internal Waves in Enclosures. *SIAM Journal of Scientific and Statistical Computing*, 5(4):958–977, December 1984. 3

[7] H.R. Baum and R.G. Rehm. Calculations of Three Dimensional Buoyant Plumes in Enclosures. *Combustion Science and Technology*, 40:55–77, 1984. 3

[8] R.G. Rehm, P.D. Barnett, H.R. Baum, and D.M. Corley. Finite Difference Calculations of Buoyant Convection in an Enclosure: Verification of the Nonlinear Algorithm. *Applied Numerical Mathematics*, 1:515–529, 1985. 3

[9] K.B. McGrattan, T. Kashiwagi, H.R. Baum, and S.L. Olson. Effects of Ignition and Wind on the Transition to Flame Spread in a Microgravity Environment. *Combustion and Flame*, 106:377–391, 1996. 4

[10] T. Kashiwagi, K.B. McGrattan, S.L. Olson, O. Fujita, M. Kikuchi, and K. Ito. Effects of Slow Wind on Localized Radiative Ignition and Transition to Flame Spread in Microgravity. In *Twenty-Sixth Symposium (International) on Combustion*, pages 1345–1352. Combustion Institute, Pittsburgh, Pennsylvania, 1996. 4

[11] W. Mell and T. Kashiwagi. Dimensional Effects on the Transition from Ignition to Flame Spread in Microgravity. In *Twenty-Seventh Symposium (International) on Combustion*, pages 2635–2641. Combustion Institute, Pittsburgh, Pennsylvania, 1998. 4

[12] W. Mell, S.L. Olson, and T. Kashiwagi. Flame Spread Along Free Edges of Thermally-Thin Samples in Microgravity. In *Twenty-Eighth Symposium (International) on Combustion*, pages 2843–2849. Combustion Institute, Pittsburgh, Pennsylvania, 2000. 4

[13] K. Prasad, Y. Nakamura, S.L. Olson, O. Fujita, K. Nishizawa, K. Ito, and T. Kashiwagi. Effect of Wind Velocity on Flame Spread in Microgravity. In *Twenty-Ninth Symposium (International) on Combustion*, pages 2553–2560. Combustion Institute, Pittsburgh, Pennsylvania, 2002. 4

[14] Y. Nakamura, T. Kashiwagi, K.B. McGrattan, and H.R. Baum. Enclosure Effects on Flame Spread over Solid Fuels in Microgravity. *Combustion and Flame*, 130:307–321, 2002. 4

[15] W.E. Mell, K.B. McGrattan, and H.R. Baum. g-Jitter Effects on Spherical Diffusion Flames. *Microgravity Science and Technology*, 15(4):12–30, 2004. 4

[16] A. Mukhopadhyay and I.K. Puri. An Assessment of Stretch Effects on Flame Tip Using the Thin Flame and Thick Formulations. *Combustion and Flame*, 133:499–502, 2003. 4

[17] A. Hamins, M. Bundy, I.K. Puri, K.B. McGrattan, and W.C. Park. Suppression of Low Strain Rate Non-Premixed Flames by an Agent. In *Proceedings of the 6th International Microgravity Combustion Workshop, NASA/CP-2001-210826*, pages 101–104. National Aeronautics and Space Administration, Lewis Research Center, Cleveland, Ohio, May 2001. 4

[18] K.B. McGrattan, R.G. Rehm, and H.R. Baum. Fire-Driven Flows in Enclosures. *Journal of Computational Physics*, 110(2):285–291, 1994. 4

[19] P. Friday and F. W. Mowrer. Comparison of FDS Model Predictions with FM/SNL Fire Test Data. NIST GCR 01-810, National Institute of Standards and Technology, Gaithersburg, Maryland, April 2001. 6

[20] A. Bounagui, N. Benichou, C. McCartney, and A. Kashef. Optimizing the Grid Size Used in CFD Simulations to Evaluate Fire Safety in Houses. In *3rd NRC Symposium on Computational Fluid Dynamics, High Performance Computing and Virtual Reality*, pages 1–8, Ottawa, Ontario, Canada, December 2003. National Research Council, Canada. 6

[21] R.L. Alpert. *SFPE Handbook of Fire Protection Engineering*, chapter Ceiling Jet Flows. National Fire Protection Association, Quincy, Massachusetts, 3rd edition, 2003. 6

[22] A. Bounagui, A. Kashef, and N. Benichou. Simulation of the Dynamics of the Fire for a Section of the L.H.-La Fontaine Tunnel. IRC-RR- 140, National Research Council Canada, Ottawa, Canada, K1A0R, September 2003. 6

[23] Y. Xin. Assessment of Fire Dynamics Simulation for Engineering Applications: Grid and Domain Size Effects. In *Proceedings of the Fire Suppression and Detection Research Application Symposium, Orlando, Florida*. National Fire Protection Association, Quincy, Massachusetts, 2004. 6

[24] J.A. Ierardi and J.R. Barnett. A Quantititive Method for Calibrating CFD Model Calculations. In *Proceedings of the CIB-CTBUH International Conference on Tall Buildings*, pages 507–514. International Council for Research and Innovation in Building and Construction (CIB), 2003. 6

[25] G. Heskestad. *SFPE Handbook of Fire Protection Engineering*, chapter Fire Plumes, Flame Height and Air Entrainment. National Fire Protection Association, Quincy, Massachusetts, 3rd edition, 2002. 6

[26] N.M. Petterson. Assessing the feasibility of reducing the grid resolution in fds field modeling. Fire Engineering Research Report 2002/6, University of Canterbury, Christchurch, New Zealand, March 2002. 6

[27] A. Musser, K. B. McGrattan, and J. Palmer. Evaluation of a Fast, Simplified Computational Fluid Dynamics Model for Solving Room Airflow Problems. NISTIR 6760, National Institute of Standards and Technology, Gaithersburg, Maryland, June 2001. 6

[28] K.B. McGrattan, S. Hostikka, J.E. Floyd, H.R. Baum, and R.G. Rehm. Fire Dynamics Simulator (Version 5), Technical Reference Guide. NIST Special Publication 1018-5, National Institute of Standards and Technology, Gaithersburg, Maryland, October 2007. 7

[29] W. Zhang, A. Hamer, M. Klassen, D. Carpenter, and R. Roby. Turbulence Statistics in a Fire Room Model by Large Eddy Simulation. *Fire Safety Journal*, 37:721–752, 2002. 7

[30] J. Smagorinsky. General Circulation Experiments with the Primitive Equations. I. The Basic Experiment. *Monthly Weather Review*, 91(3):99–164, March 1963. 7

[31] J.W. Deardorff. Numerical Investigation of Neutral and Unstable Planetary Boundary Layers. *Journal of Atmospheric Sciences*, 29:91–115, 1972. 7

[32] M. Germano, U. Piomelli, P. Moin, and W.H. Cabot. A Dynamic Subgrid-Scale Eddy Viscosity Model. *Physics of Fluids A*, 3(7):1760–1765, 1991. 7

[33] D.K. Lilly. A Proposed Modification of the Germano Subgrid-Scale Closure Method. *Physics of Fluids A*, 4(3):633–635, 1992. 7

[34] J. Hietaniemi, S. Hostikka, and J. Vaari. FDS Simulation of Fire Spread – Comparison of Model Results with Experimental Data. VTT Working Papers 4, VTT Building and Transport, Espoo, Finland, 2004. 8

[35] C. Lautenberger, G. Rein, and C. Fernandez-Pello. The application of a genetic algorithm to estimate the material properties for fire modeling from bench-scale fire test data. *Fire Safety Journal*, 41:204–214, 2006. 8

[36] J.C. Adams, W.S. Brainerd, J.T. Martin, B.T. Smith, and J.L. Wagener. *Fortran 95 Handbook: Complete ISO/ANSI Reference*. MIT Press, Cambridge, Massachusetts, 1997. 9

[37] R. Siegel and J. R. Howell. *Thermal Radiation Heat Transfer*. Taylor & Francis, New York, 4th edition, 2002. 11, 12

[38] Y.B. Zel'dovich and Y.P. Raizer. *Physics of shock waves and high-temperature hydrodynamic phenomena*. Dover Publications, New York, 2002. Translated from the Russian and then edited by W.D.Hayes and R.F. Probstein. 13, 14

[39] D. Drysdale. *An Introduction to Fire Dynamics*. John Wiley and Sons, New York, 2nd edition, 2002. 16

[40] H.S. Carslaw and J.C. Jaegar. *Conduction of Heat in Solids*. Oxford University Press, 2nd edition, 1959. 16

[41] K.W. Childs. HEATING 7: Multidimensional, Finite-Difference Heat Conduction Analysis Code System. Technical Report PSR-199, Oak Ridge National Laboratory, Oak Ridge, TN, 1998. 17